

1 **Supplementary Material**

2 **Atomic modulation and phase engineering of MoS₂ for boosting**

3 **N₂ reduction**

4
5 **Yansong Jia^{1,2,#}, Guining Shao^{1,2,#}, Yang Li^{1,2}, Ruizhe Yang³, Ming Huang³, Hua Huang⁴, Min Liu⁵,**
6 **Gai Huang⁴, Qunjie Lu⁴, Chaohua Gu^{1,2}**

7
8 ¹Institute of Process Equipment, College of Energy Engineering, Zhejiang University, Hangzhou 310000, Zhejiang,
9 China.

10 ²Hydrogen Energy Institute, Zhejiang University, Hangzhou 310000, Zhejiang, China.

11 ³Institute of Fundamental and Frontier Sciences, University of Electronic Science and Technology of China,
12 Chengdu 611731, Sichuan, China.

13 ⁴National energy key laboratory for new hydrogen-ammonia energy technologies, Foshan Xianhu Laboratory,
14 Foshan 528200, Guangdong, China.

15 ⁵State Grid Zhejiang Electric Power CO., LTD. Research Institute, Hangzhou 310000, Zhejiang, China.

16 #Authors contributed equally.

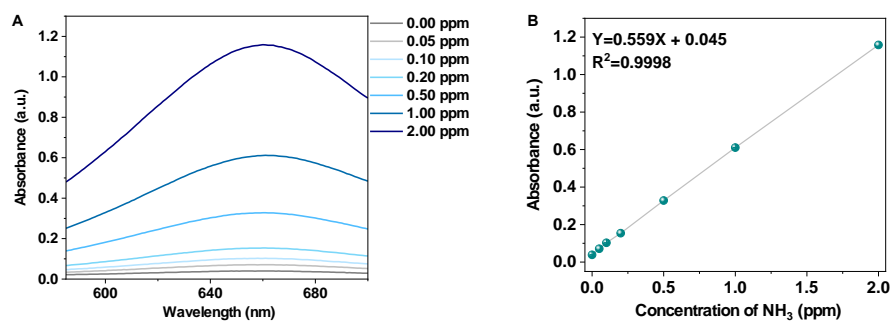
17 18 **Characterization methods**

19 The phase data were analyzed by X-ray powder diffraction (XRD) on an MMA diffractometer equipped
20 with Cu K α radiation (GBC, MMA), which operated from 10° to 80° in continuous scan mode with a
21 scan rate of 1° min⁻¹. X-ray photoelectron spectroscopy (XPS) experiments were carried out on a VG
22 Scientific ESCALAB 2201XL instrument using aluminum K α X-ray radiation. X-ray absorption studies
23 (XAS) were performed at the BL11B beamline at the Shanghai Synchrotron Radiation Facility (SSRF),
24 Shanghai, PR China. Raman spectra were collected on a JOBIN YVON HR800 Confocal Raman System
25 with 632.8 nm diode laser excitation on a 300 lines mm⁻¹ grating under ambient conditions. The specific
26 surface areas were determined using the Brunauer-Emmett-Teller (BET, Micro for TriStar II Plus 2.02)
27 method, with a degassing pretreatment of N₂ at 200 °C for 24 h. The structure and morphology of the
28 sample were investigated on a field emission scanning electron microscope (FESEM; JEOL JSM-7500)
29 and a transmission electron microscope (TEM; JEOL-2010). Atomic resolution analytical microscope
30 investigations were conducted using scanning TEM (STEM; JEOL ARM 200F), which was operated at
31 80 kV and equipped with a cold field emission high-resolution pole piece and a Centurio energy
32 dispersive spectroscopy (EDS) detector. The electrochemical operando ATR-SEIRAS was measured by
33 INVENIO R FTIR spectrometer (Bruker) equipped with a mercury-cadmium-telluride (MCT) detector.



© The Author(s) 2021. Open Access This article is licensed under a Creative Commons Attribution 4.0 International License
(<https://creativecommons.org/licenses/by/4.0/>), which permits unrestricted use, sharing, adaptation, distribution and reproduction in any medium or

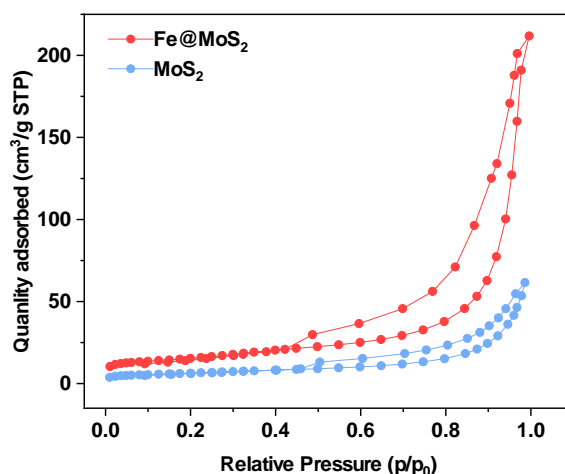
format, for any purpose, even commercially, as long as you give appropriate credit to the original author(s) and the source, provide a link to the Creative Commons license, and indicate if changes were made.



35

36 **Supplementary Figure 1.** Standard curves. (A) UV-Vis absorption spectra of NH_3 standard solutions;
 37 (B) Calibration curve for colorimetric NH_3 assay using salicylic acid.

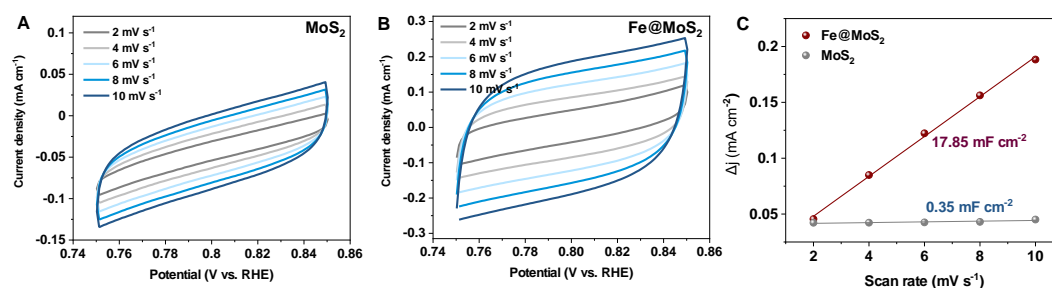
38



39

40 **Supplementary Figure 2.** N_2 adsorption and desorption isotherms of MoS_2 and Fe@MoS_2 .

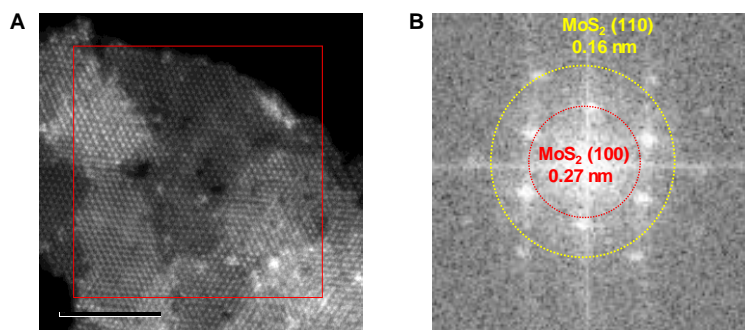
41



42

43 **Supplementary Figure 3.** CV curves of (A) MoS_2 , (B) Fe@MoS_2 at potential from 0.75 V to 0.85 V at a
 44 scan rate of 2, 4, 6, 8, 10 mV s^{-1} . (C) The measured capacitive currents are plotted as a function of the
 45 scan rate.

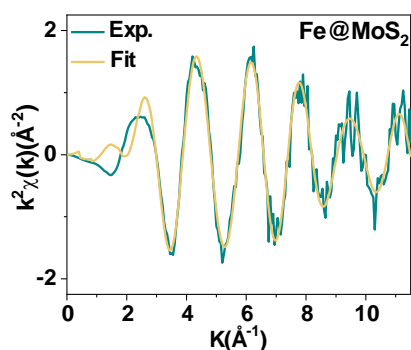
46



47

48 **Supplementary Figure 4.** STEM image of A) Fe@MoS₂, and B) the corresponding Fourier transform.

49

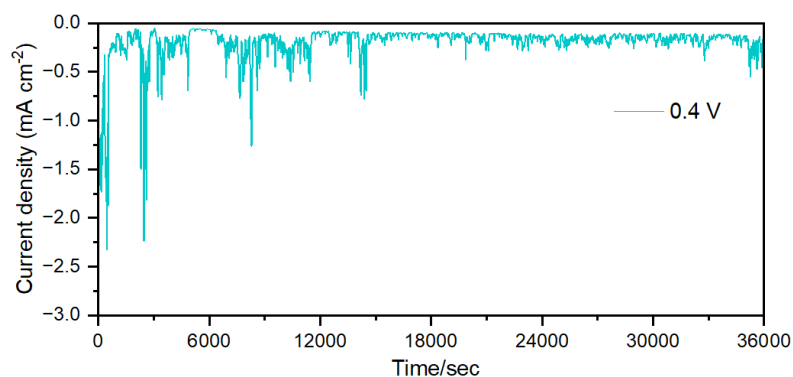


50

51 **Supplementary Figure 5.** The corresponding EXAFS fitting curves of Fe@MoS₂.

52

53



54

55 **Supplementary Figure 6.** Long-term stability test of Fe@MoS₂.

56

57 **Supplementary Table 1.** BET surface area and pore volume of ENRR catalysts.

ENRR catalysts	MoS ₂	Fe@MoS ₂
Specific area (m ² g ⁻¹)	22.63	54.034
Pore volume (cm ³ g ⁻¹)	0.09	0.32

58

59 **Supplementary Table 2.** Fe *K*-edge EXAFS curve Fitting Parameter.

Sample	Path	C.N.	R (Å)	σ ² ×10 ³ (Å ²)	R factor
--------	------	------	-------	---	----------

Fe Foil	Fe-Fe1	8.0	1.96±0.03	2.3±0.5	0.004
	Fe-Fe2	6.0	2.67±0.01	2.3±0.5	
Fe@MoS ₂	Fe-S	5.5±0.4	2.29±0.05	3.3±0.7	0.004
	Fe-Mo	0.7±0.1	2.83±0.025	1.9±0.5	

60

61 **Supplementary Table 3.** Comparison of ENRR performance.

Catalysts	Electrolyte	Yield Rate	FE (%)	Ref
Fe@MoS ₂	0.25 M LiClO ₄	20.20 μg h ⁻¹ mg ⁻¹	19.7%	This work
MoS ₂ /BCCF	0.1 M Li ₂ SO ₄	43.4 μg h ⁻¹ mg ⁻¹	9.81%	[1]
MoS ₂ /C ₃ N ₄	0.1 M Na ₂ SO ₄	19.86 μg h ⁻¹ mg ⁻¹	6.87%	[2]
Cu _{2-x} S/MoS ₂	0.1 M Na ₂ SO ₄	22.1 μg h ⁻¹ mg ⁻¹	6.06%	[3]
SnS ₂ /MoS ₂	0.1 M Li ₂ SO ₄	34.3 μg h ⁻¹ mg ⁻¹	13.8%	[4]
V _S -MoS ₂	0.1 M Na ₂ SO ₄	29.55 μg h ⁻¹ mg ⁻¹	4.58%	[5]
VS-Fe-MoS ₂ /C	0.1 M LiClO ₄	17.8 μg h ⁻¹ mg ⁻¹	9.2%	[6]
Fe-MoS ₂ /CC	0.1 M KOH	12.5 μg h ⁻¹ mg ⁻¹	10.5%	[7]
MoS ₂ NDs/RGO	0.1 M Na ₂ SO ₄	16.41 μg h ⁻¹ mg ⁻¹	27.93%	[8]
MoS ₂ -rGO	0.1 M LiClO ₄	24.82 μg h ⁻¹ mg ⁻¹	4.58%	[9]
MoS ₂ /CC	0.1 M Na ₂ SO ₄	5.23 μg h ⁻¹ mg ⁻¹	1.17%	[10]

62

63 **REFERENCES**

- 64 1. Liu Y, Han M, Xiong Q, Zhang S, Zhao C, et al. Dramatically Enhanced Ambient Ammonia
65 Electrosynthesis Performance by In-Operando Created Li-S Interactions on MoS₂ Electrocatalyst. *Adv*
66 *Energy Mater* 2019;9:1803935. <https://doi.org/10.1002/aenm.201803935>
- 67 2. Zhao Z, Luo S, Ma P, Luo Y, Wu W, et al. In Situ Synthesis of MoS₂ on C₃N₄ To Form MoS₂/C₃N₄
68 with Interfacial Mo-N Coordination for Electrocatalytic Reduction of N₂ to NH₃. *ACS Sustainable Chem*
69 *Eng* 2020;8:8814-22. <https://doi.org/10.1021/acssuschemeng.0c02763>
- 70 3. Jiang T, Li L, Li L, Liu Y, Zhang D, et al. Ultra-thin shelled Cu_{2-x}S/MoS₂ quantum dots for
71 enhanced electrocatalytic nitrogen reduction. *Chem Eng J* 2021;426:130650.
72 <https://doi.org/10.1016/j.cej.2021.130650>
- 73 4. Xiang L, Liu S, Zhao L, Yuan S, Li X, et al. Modifying the electronic structure of MoS₂ via
74 interface engineering to boost intrinsic activity for nitrogen fixation. *J Alloys Compd* 2023;945:169201.
75 <https://doi.org/10.1016/j.jallcom.2023.169201>
- 76 5. Ma C, Yan X, He H, Liu B, Yan S. A defective MoS₂ monolayer as an efficient electrocatalyst for
77 the nitrogen reduction reaction: a combined theoretical and experimental study. *Sustainable Energy Fuels*
78 2021;5:2415-8. <https://doi.org/10.1039/D1SE00346A>
- 79 6. He Z, Jiang Y, Cui X, Liu Z, Meng X, et al. Fe-Doped 1T/2H Mixed-Phase MoS₂/C Nanostructures
80 for N₂ Electroreduction into Ammonia. *ACS Appl Nano Mater* 2022;5:5470-8.
81 <https://doi.org/10.1021/acsnm.2c00467>
- 82 7. Zhao X, Zhang X, Xue Z, Chen W, Zhou Z, et al. Fe nanodot-decorated MoS₂ nanosheets on carbon
83 cloth: an efficient and flexible electrode for ambient ammonia synthesis. *J Mater Chem A*

- 84 2019;7:27417-22. <https://doi.org/10.1039/C9TA09264A>
- 85 8. Liu Y, Wang W, Zhang S, Li W, Wang G, et al. MoS₂ Nanodots Anchored on Reduced Graphene
86 Oxide for Efficient N₂ Fixation to NH₃. *ACS Sustainable Chem Eng* 2020;8:2320-6.
87 <https://doi.org/10.1021/acssuschemeng.9b07679>
- 88 9. Li X, Ren X, Liu X, Zhao J, Sun X, et al. A MoS₂ nanosheet–reduced graphene oxide hybrid: an
89 efficient electrocatalyst for electrocatalytic N₂ reduction to NH₃ under ambient conditions. *J Mater*
90 *Chem A* 2019;7:2524-8. <https://doi.org/10.1039/C8TA10433F>
- 91 10. Zhang L, Ji X, Ren X, Ma Y, Shi X, et al. Electrochemical Ammonia Synthesis via Nitrogen
92 Reduction Reaction on a MoS₂ Catalyst: Theoretical and Experimental Studies. *Adv Mater*
93 2018;30:1800191. <https://doi.org/10.1002/adma.201800191>
- 94